



ELSEVIER

Available online at [www.sciencedirect.com](http://www.sciencedirect.com)

SCIENCE @ DIRECT®

Journal of Sound and Vibration 282 (2005) 1208–1220

JOURNAL OF  
SOUND AND  
VIBRATION

[www.elsevier.com/locate/jsvi](http://www.elsevier.com/locate/jsvi)

Short Communication

# Identifying Coulomb and viscous damping from free-vibration acceleration decrements

Jin-Wei Liang\*

*Department of Mechanical Engineering, Ming-Chi University of Technology, Taipei 24306, Taiwan*

Received 16 January 2004; received in revised form 26 March 2004; accepted 19 April 2004

Available online 28 October 2004

---

## Abstract

A new damping-identification method for the simultaneous identification of Coulomb and viscous damping effects from free-vibration acceleration decrements in a damped linear single degree-of-freedom (dof) mass-spring system is presented. In deriving the algorithms, the governing differential equations are solved to come up with two schemes separately suitable for viscous and dry-friction damping estimations. Numerical study of a combined-damping system demonstrates a perfect match between the estimated values and the simulation parameters. The method is also applied to an experimental system. Experimental estimates obtained from the proposed method are compared to those obtained using other identification schemes to illustrate the effectiveness and reliability of the new method.

© 2004 Elsevier Ltd. All rights reserved.

---

## 1. Introduction

At times the amount of damping in a given system is not known and must be determined experimentally. When considering the case in which damping is viscous and the system is underdamped, viscous damping will cause the vibration to decay exponentially, where the exponent is a linear function of the damping factor  $\zeta$ . The logarithmic decrement method, originally proposed by Helmholtz [1] and later on introduced by Lord Rayleigh [2], can be adopted to determine the amount of viscous damping experimentally. The method postulates that the

---

\*Tel.: +886-2-29089899; fax: +886-2-29041914.

*E-mail address:* [liangj@ccsun.mit.edu.tw](mailto:liangj@ccsun.mit.edu.tw) (J.-W. Liang).

difference in the logarithms of successive excursions is nearly constant. When dealing with a vibration system having a mass and spring with Coulomb friction, Lorenz [3] first noticed that the successive extreme excursions in the system decreases at a constant rate. From this property, one can extract Coulomb friction from the constant decrement of a harmonic oscillator with constant frictional damping.

Nevertheless, many machines and structures have both sources of damping. To deal with such cases, Jacobsen and Ayre [4] developed an approximate scheme to estimate both parameters from free-vibration decrements and found that the viscous friction dominates in the large-amplitude responses, whereas Coulomb friction dominates in the small-amplitude oscillations. Watari [5] proposed an exact estimation scheme, which went unnoticed beyond the Japanese-speaking community until it was recently re-derived in Ref. [6] and applied to an industrial linear-bearing system in Ref. [7].

This study bases on Ref. [6] and proposes a damping-identification method using the acceleration decrements. The method is especially suitable for the cases in which displacement measurements are unfeasible, but acceleration measurements are available, for example with accelerometers. In addition, systems with solely viscous damping or dry friction can be treated as special cases of this study.

Many real systems may exhibit frictional characteristics other than “viscous plus Coulomb” model. These friction characteristics may include those pertaining to contact compliance [8–11], unsteady friction–velocity relationship such as Stribeck friction [12,13], state-variable friction [14,15], and the LuGre dynamic friction model [9,16]. The method developed here does not attempt to account for these dynamical behaviors.

## 2. Free vibration with Coulomb and viscous damping

This paper considers a mass–spring–dashpot system with a dry-friction contact, for which, based on Newton’s second law, the equation of motion is

$$m\ddot{x} + c\dot{x} + kx + f(\dot{x}) = 0, \tag{1}$$

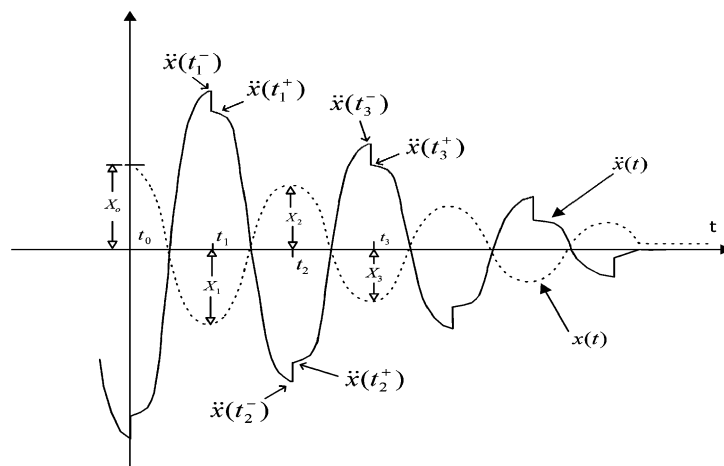


Fig. 1. A schematic diagram depicting the displacement and acceleration responses of the frictional oscillator.

where  $x$  is the displacement of the mass from the unstretched position.  $m$ ,  $c$ , and  $k$  are the mass, viscous-damping coefficient, and stiffness, respectively. The dry friction has the form  $f(\dot{x}) = f_k \operatorname{sgn}(\dot{x})$ ,  $\dot{x} \neq 0$ , and  $-f_s \leq f(0) \leq f_s$ . One can loosely refer to  $f(\dot{x})$  as Coulomb friction [6].

Fig. 1 shows a schematic diagram depicting the free-vibration displacement and acceleration responses of a single degree-of-freedom (dof) vibration system. Referring to Fig. 1 and assuming that the system starts with  $x(t_0) = X_0 > x_s$  (here,  $x_s = f_s/k$ ), and  $\dot{x}(t_0) = 0$ , then the motion proceeds with  $\dot{x} < 0$ . The response of the system has the following form [6]:

$$x(t) = (X_0 - x_k)e^{-\zeta\omega_n(t-t_0)}(\cos \omega_d(t - t_0) + \beta \sin \omega_d(t - t_0)) + x_k, \tag{2}$$

where  $\omega_n = k/m$ ,  $2\zeta\omega_n = c/m$ ,  $x_k = f_k/k$ ,  $\omega_d = \omega_n\sqrt{1 - \zeta^2}$ , and  $\beta = \zeta/\sqrt{1 - \zeta^2}$ . In addition, the acceleration response corresponding to the same interval is

$$\ddot{x}(t) = \frac{\omega_n}{\sqrt{1 - \zeta^2}}(X_0 - x_k)e^{-\zeta\omega_n(t-t_0)}\{\zeta\omega_n \sin \omega_d(t - t_0) - \omega_d \cos \omega_d(t - t_0)\}. \tag{3}$$

Eqs. (2) and (3) are valid until  $\dot{x} = 0$ , at which time  $t = t_1 = t_0 + \pi/\omega_d$ ,  $X_1 = x(t_1) = -e^{-\beta\pi}X_0 + (1 + e^{-\beta\pi})x_k$  and  $\ddot{x}(t_1^-) = \omega_n^2(X_0 - x_k)e^{-\beta\pi}$ .

If  $X_1 < -x_s$ , then the mass will reverse direction and continue sliding with  $\dot{x} > 0$ . The displacement and acceleration corresponding to this interval are [6]

$$x(t) = (X_1 + x_k)e^{-\zeta\omega_n(t-t_1)}\{\cos \omega_d(t - t_1) + \beta \sin \omega_d(t - t_1)\} - x_k \tag{4}$$

and

$$\ddot{x}(t) = \frac{-\omega_n}{\sqrt{1 - \zeta^2}}(X_1 + x_k)e^{-\zeta\omega_n(t-t_1)}\{-\zeta\omega_n \sin \omega_d(t - t_1) + \omega_d \cos \omega_d(t - t_1)\}. \tag{5}$$

Thus, at  $t = t_1^+$ ,  $\ddot{x}(t_1^+) = -\omega_n^2(X_1 + x_k)$  according to Eq. (5). Eqs. (4) and (5) are valid until  $\dot{x} = 0$  again, at which time  $t = t_2 = t_1 + \pi/\omega_d$ ,  $X_2 = x(t_2) = -e^{-\beta\pi}X_1 - (1 + e^{-\beta\pi})x_k$  and  $\ddot{x}(t_2^-) = \omega_n^2(X_1 + x_k)e^{-\beta\pi}$ . If  $X_2 > x_s$ , motion will continue.

This process can be iterated until  $-x_s \leq X_n \leq x_s$ , at which time the motion stops. The iterated process leads to a recursive relation for the successive displacement peaks and valleys in the oscillatory response [6,7]:

$$X_i = -e^{-\beta\pi}X_{i-1} + (-1)^{i-1}(e^{-\beta\pi} + 1)x_k, \quad i = 1, 2, \dots, n. \tag{6}$$

From the evolution of decaying displacement peaks and valleys presented in Eq. (6), one can isolate the viscous effect. Then, the following two identification equations based on displacement decrements can be achieved [6,7]:

$$(X_{i+1} + X_i)/(X_i + X_{i-1}) = -e^{-\beta\pi}, \tag{7}$$

$$(X_{i+1} - X_{i-1})/(X_i - X_{i-2}) = -e^{-\beta\pi}. \tag{8}$$

In Ref. [6], an identification scheme was proposed which applies either Eqs. (7) or (8), depending on the data features, for the determination of the viscous-damping parameter,  $\beta$ , and then extract the Coulomb effect from Eq. (6) together with the knowledge of  $\beta$ . This identification process was denoted as the displacement-decrement method for the combined-damped system.

The iteration process also gives rise to the following expressions of acceleration magnitudes. These acceleration magnitudes can be quantified at the instants “before” and “after” each

individual jump, i.e.,

$$\begin{aligned} \ddot{x}(t_j^-) &= \omega_n^2(X_{j-1} - x_k)e^{-\beta\pi}, \\ \ddot{x}(t_j^+) &= -\omega_n^2(X_j + x_k), \quad j \text{ is odd} \end{aligned} \tag{9}$$

and

$$\begin{aligned} \ddot{x}(t_j^-) &= \omega_n^2(X_{j-1} + x_k)e^{-\beta\pi}, \\ \ddot{x}(t_j^+) &= \omega_n^2(x_k - X_j), \quad j \text{ is even.} \end{aligned} \tag{10}$$

If one works with the acceleration expressions presented in Eqs. (9) and (10) together with the recursive relationships developed in Eqs. (6)–(8), one can come up with the following identification equations:

$$\ddot{x}(t_j^-) - \ddot{x}(t_j^+) = 2(-1)^{j+1}\omega_n^2x_k, \tag{11}$$

$$\frac{\ddot{x}(t_{j+2}^-) - \ddot{x}(t_j^-)}{\ddot{x}(t_{j+1}^-) - \ddot{x}(t_{j-1}^-)} = -e^{-\beta\pi}, \tag{12}$$

$$\frac{\ddot{x}(t_j^+) + \ddot{x}(t_{j+1}^+)}{\ddot{x}(t_{j-1}^+) + \ddot{x}(t_j^+)} = -e^{-\beta\pi}. \tag{13}$$

Evidently, if the system’s natural frequency is known, Eq. (11) can be adopted to estimate the dry-friction parameter,  $x_k$ , by using a single-acceleration jump. In contrast, the viscous-damping parameter,  $\beta$ , can be estimated from ratios of acceleration differences as depicted in Eqs. (12) and (13). There are two kinds of acceleration differences involved in Eqs. (12) and (13). One of them measures the differences between the acceleration magnitudes at instants before every other acceleration jump, namely “ $\ddot{x}(t_{j+2}^-) - \ddot{x}(t_j^-)$ ” or “ $\ddot{x}(t_{j+1}^-) - \ddot{x}(t_{j-1}^-)$ ”, whereas another one measures the difference between magnitudes corresponding to instants immediately after successive acceleration jumps, i.e., “ $\ddot{x}(t_j^+) + \ddot{x}(t_{j+1}^+)$ ” or “ $\ddot{x}(t_{j-1}^+) + \ddot{x}(t_j^+)$ ”. All of these expressions denote acceleration differences although two of them actually involve a “plus” sign. Finally, either Eq. (12) or (13) can be applied to estimate  $\beta$ .

As described previously, to implement the displacement-decrement method proposed in Refs. [6,7], either Eq. (7) or (8) can be utilized for the determination of the viscous-damping parameter  $\beta$  (and  $\zeta$ ). Then the dry-friction parameter  $x_k$  is extracted from Eq. (6) together with the estimated value of  $\zeta$ . As such, errors in the estimate of  $\zeta$  could be propagated into the estimate of  $x_k$ . In the acceleration-decrement method, the  $\zeta$  and  $x_k$  estimations are identified from two separate equations. Hence, damping quantities can be calculated simultaneously, and the accuracy of one estimate will not affect that of another. Based on this, it is conceivable that the acceleration-decrement method could be a better choice in comparison with the displacement-decrement method if the estimating accuracy is of concern and the acceleration measurements are accurate enough. In order to verify the reliability and effectiveness of the proposed identification schemes, numerical simulations are carried out in the next section by assuming that only acceleration signal is feasible.

### 3. Numerical example

Note that many numerical studies on systems with damping to different degrees were performed, the identification accuracy obtained were quite consistent. However, to simplify the presentation, only one simulation example is elaborated below. In this numerical example, Eq. (1) was integrated with the parameter values  $m = 1.0$ ,  $k = 100.0$ ,  $c = 1.0$ , and  $f_k = 3.0$ . Based on these values,  $\omega_n = 10.0$ ,  $\zeta = 0.05$ , and  $x_k = 0.03$ . The initial conditions in this example were  $x(0) = 1.0$  and  $\dot{x}(0) = 0$ . The damping of the system was intentionally chosen to be light enough to acquire sufficiently many free oscillations. The numerical integration algorithm followed that of Refs. [6,7], carefully accounting for the discontinuous switching in the friction. To do so, one needed to check whether the velocity has changed sign, and iterating to precisely determine the time of direction reversal. Similar algorithms were discussed in Refs. [17,18], and others in Refs. [19,20].

Under these conditions, the simulated responses approximately went through four complete periods of damped free oscillation prior to the occurrence of sticking. Based on the simulated data and the identification schemes described in Eqs. (11)–(13), one can obtain accurate dry-friction and viscous-damping estimates. For instance, the maximum inaccuracy of the dry-friction estimation was about 1%, occurring at the first acceleration jump. The same inaccuracy decreased to about 0.3% at the fifth acceleration jump. Thus, the accuracy of dry-friction damping estimation was high, and it improved as the magnitudes of the acceleration response decreased. In contrast, the accuracy of viscous-damping estimate seemed to be less sensitive to the locations of the response. For example, the inaccuracy of viscous-damping estimate, whether calculated from the first or last couple cycles of acceleration response, was about 0.1%. Compared with the dry-friction estimation, the viscous-damping had a slightly better accuracy. This trend agreed with the observations made previously in Refs. [6,7].

In order to understand whether the proposed idea works in a real system, the new identification schemes is further examined on an experimental system in the next section. The damping source engaged to this system is controllable. Therefore, the experimental system can be tuned to be a viscous-, Coulomb-, or combined-damped system.

## 4. Experimental validations

### 4.1. The experimental system

The experimental system adopted in this study is basically the same as that of Ref. [6]. The only difference is that in addition to the displacement-measurement device, here, an accelerometer (PCB Model 393C) was used to measure the acceleration response. The accelerometer adopted had a workable frequency range from 0.025 to 800 Hz with a 5% transverse sensitivity. The nominal sensitivity of the accelerometer was 1 V/g with a resonant frequency of 3.5 kHz. Features of this experimental system included that the mass, consisting mainly of the accelerometer's mass, glided in an air track. An eddy-current damper was employed to provide a nearly linear damping characteristic. The amount of the viscous damping applied to the system was adjustable. Finally, a

dry-friction contact was created by packing paper between the electromagnets and the steel flange of the eddy-current damper. Details regarding this experimental system can be found in Ref. [6].

Despite the assumption of the unfeasibility of displacement measurement made in the previous section, both the displacement and acceleration decrements would be measured in the experimental study to crosscheck the identification results acquired using the proposed method. Additionally, while only typical experimental cases are presented in this study, many other experiments and identifications were carried out, and the results, especially the identification accuracy, are quite consistent with what will be presented below.

#### 4.2. The isolated damping cases

To provide some basis of evaluating the identification results, the isolated effects of each type of damping were first estimated. Among which, the viscous-damping ratio  $\zeta$  could be determined by using the logarithmic decrement method while removing the dry-friction contact. Similarly, the dry-friction effect,  $x_k$ , could be estimated when the eddy-current damper was switched off. To that end, Fig. 2 illustrates the free-vibration responses with viscous-damping acting alone, while Fig. 3 demonstrates the case where dry friction is the only active damping source.

In Figs. 2 and 3, the initial conditions were generated by first displacing the sliding mass and holding it still, then suddenly releasing it. The releasing action was taken with much precaution to avoid the presence of any sources of disturbance. However, since it is difficult to release the mass perfectly instantly, the possibility that the imperfect releasing might distort the response in a slight-damping case cannot be completely excluded. Nonetheless, the responses presented in Figs. 2 and 3 show that while slight distortion appears in the beginning of the signal, during the rest of time, the mass seems to move nicely and freely. The estimation procedure is applicable to a single dof from velocity reversal to velocity reversal. Once a velocity reversal takes place, the

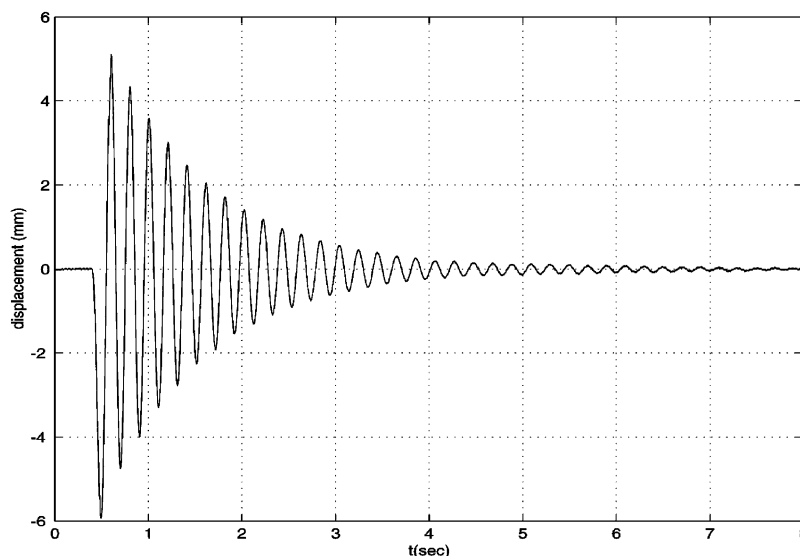


Fig. 2. The free response with eddy-current damping alone (dry friction removed) depicts a logarithmic decrement.

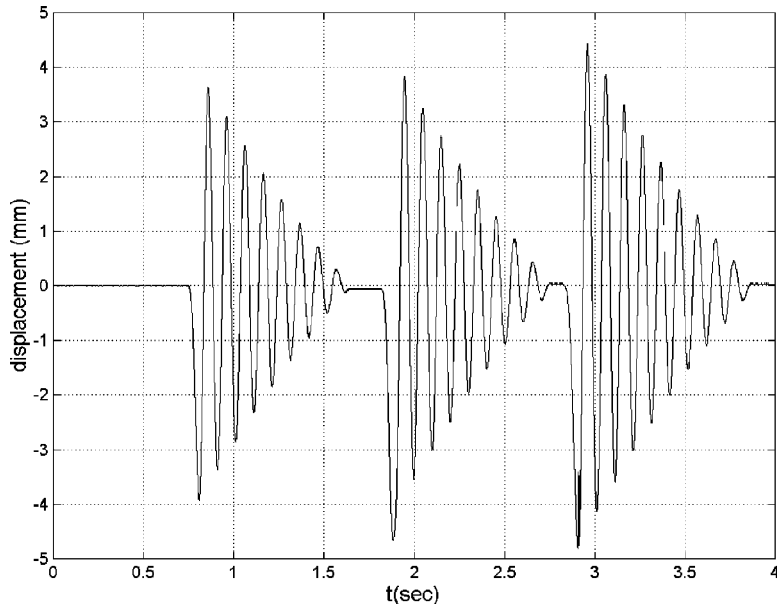


Fig. 3. The free response with dry friction alone (eddy-current switched off) indicates a nearly constant decrement.

subsequent motion is suitable for the procedure, regardless of the initial conditions prior to the first velocity reversal as long as they are sufficient to produce several periods of oscillation. To that end, in the proceeding investigations, only the first period of data will be discarded.

From Fig. 2, a cumulative logarithmic decrement was applied to the first 15 periods of data. The first period of data was discarded because it might be involved in imperfect releasing. Therefore, the data fed to the identification process started from the second period. Here, the cumulative logarithmic-decrement scheme, determining the system damping from the amplitude ratio of the first to fifteenth peak (or valley), has a beneficial averaging effect. As a consequence, the  $\zeta$  estimate for the peak decrement was 0.0298, whereas the estimate for the valley decrement was 0.0297. The averaged estimate of  $\zeta$  obtained for the whole set of data was 0.0298. This value will be denoted as  $\zeta_{\text{ref}}$  hereafter.

Next, the constant decrement criterion was applied to extract dry-friction information from Fig. 3. The data presented in Fig. 3 was measured when the dry-friction contact was engaged and the eddy-current damper was switched off. Similar to the isolated viscous-damping case, a cumulative decrement scheme was applied to the data shown in Fig. 3. Also, to avoid the imperfect releasing effects, the first period of data was discarded. There were three individual tests involved in Fig. 3, and two dry-friction estimates could be identified from each test. These estimates were calculated from the decrements of peak and valley, respectively. Hence, totally, six dry-friction estimates were calculated from Fig. 3. The resultant  $x_k$  estimates were 0.1471, 0.1461, 0.1454, 0.1450, and 0.1454. It can be seen that these estimates were consistent, with a standard deviation equal to 1%. The averaged value of  $x_k$  was equal to 0.1456, which will be denoted as  $x_{k\text{ref}}$ .

Note that both  $x_{k\text{ref}}$  and  $\zeta_{\text{ref}}$  will be used as references to evaluate whether the proposed acceleration decrement method works effectively. Additionally, based on the identification

process described above, it was found that when cumulative decrement schemes were applied, the estimates of both  $x_k$  and  $\zeta$  were quite consistent. In the next section, the proposed acceleration-decrement method will be applied to a set of combined-damping data obtained from a real system. Then, the identified results are crosschecked using the displacement-decrement method to show the reliability of the proposed method.

#### 4.3. The acceleration decrement identifications

To validate the proposed acceleration decrement method, tests involving both viscous and dry-friction damping were conducted. During the combined-damping tests, the amounts of damping applied to the system were kept to be the same as those individually applied to the isolated-damping tests. Many tests were conducted while some typical free responses including the acceleration and displacement measurements are presented in Fig. 4. There were five different tests involved in Fig. 4 which would be examined when the acceleration-decrement method was validated. In each of these five tests, at least three effective cycles of data are present.

According to the proposed schemes, the identification process would ask for magnitudes corresponding to instants immediately before and after each acceleration jump, i.e.,  $\ddot{x}(t_j^-)$  and  $\ddot{x}(t_j^+)$ . However, due to the accelerometer's sensitivity, the acceleration measurements were concealed by some high-frequency noise which made the determinations of  $\ddot{x}(t_j^+)$  and  $\ddot{x}(t_j^-)$  difficult. To overcome this, a five-point moving average process was applied to the acceleration signal. The moving average process, qualitatively equivalent to a low-passed filter, could

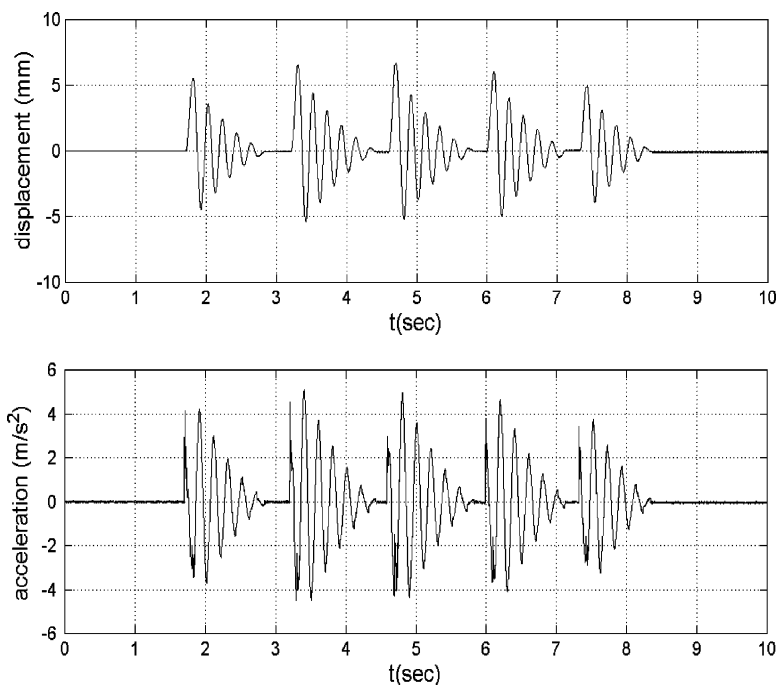


Fig. 4. The free-vibration displacement (upper plot) and acceleration (lower plot) decrements of the experimental system with both eddy-current and dry damping engaged.



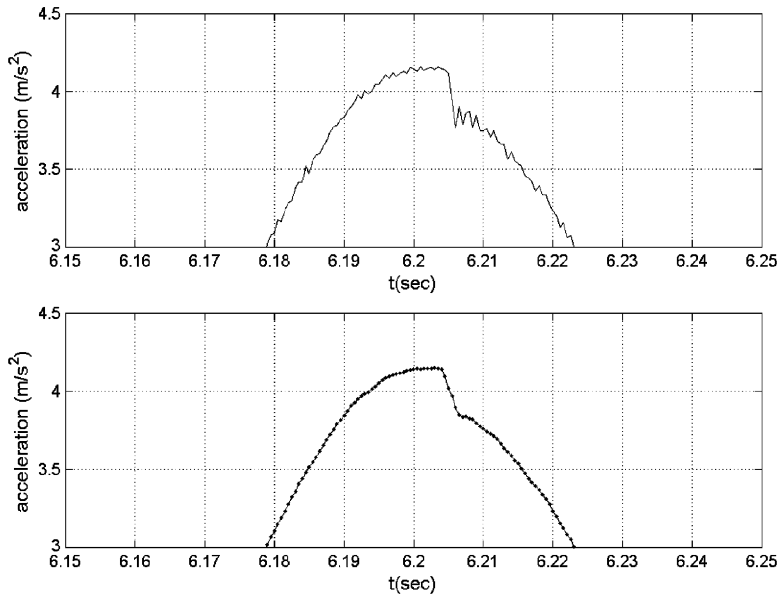


Fig. 5. A comparison between the original (upper plot) and smoothed (lower plot) acceleration jumps.

smoothen the fluctuation associated with the acceleration signal. Thus, Fig. 5 presents the original and smoothed acceleration signals in which a satisfactory smoothing effect achieved at the vicinity of abrupt acceleration change can easily be seen. Note that the effects induced by the smoothing process on the identification results are difficult to be figured out. However, it can be observed from Fig. 5 that the smooth process can help one to quickly locate the time instants at which the abrupt acceleration jumps occur. Meanwhile, the high accuracy of the damping estimate obtained using the smooth data, which will be shown later, more or less implies that the smooth process does not harm the identification process greatly.

Hence, the identification schemes listed in Eqs. (11)–(13) were applied to estimate the damping parameters using the smoothed acceleration signal. There were five individual tests involved in Fig. 4, and each test contained at least three complete cycles of responses. The natural frequency of the real vibratory system was estimated to be 30.90 rad/s, which would be needed in calculating the dry-friction estimates. Again, to avoid transient effects, one should neglect the first period of data of each test. To identify the dry-friction parameter,  $x_k$ , Eq. (11) was applied to each acceleration jump (except those pertained to initial conditions) of Fig. 4. Next, a single averaged value,  $\hat{x}_k$ , was calculated for each test. Therefore, totally five different  $\hat{x}_k$  estimates were come up with from Fig. 4, which are presented in Table 1. In Table 1, the hatted quantities indicate the estimates obtained using the acceleration-decrement method, whereas the asterisked quantities denote the results obtained from the displacement-decrement method that will be addressed later. The  $\hat{x}_k$  values listed in Table 1 are consistent, with an average equal to 0.152 (denoted as  $\hat{x}_{k\text{avg}}$ ) and a standard deviation of 1.14%. Furthermore, this averaged value is close to the reference one that obtained from the isolated-damping test, i.e.  $x_{k\text{ref}} = 0.1456$ . The error of  $\hat{x}_{k\text{avg}}$  based on the reference value,  $x_{k\text{ref}}$ , is 5.1%.

Table 1  
Experimental estimates of damping parameters

	Test 1	Test 2	Test 3	Test 4	Test 5	Average values	Reference values	Standard deviations (%)	Error (%)
$\hat{x}_k$	0.153	0.151	0.152	0.155	0.150	0.152	0.1456	1.14	5.1
$\hat{\zeta}$	0.0301	0.0324	0.0315	0.0324	0.0337	0.0320	0.0298	3.72	7.5
$x_k^*$	0.180	0.166	0.131	0.164	0.161	0.160	0.1456	10.1	10.2
$\zeta^*$	0.0316	0.0320	0.0317	0.0284	0.0298	0.0307	0.0298	4.51	3.0

Quantities with “hat” and “asterisk” correspond to estimates under combined damping obtained from the acceleration- and displacement-decrement methods, respectively. The reference quantities correspond to estimates under a single damping source.

On the other hand, in order to estimate  $\zeta$ , one could use either Eq. (12) or (13). Here, we applied both, therefore, eight different  $\zeta$  estimates were calculated for each test shown in Fig. 4. Again, the smoothed data were adopted. Next, one single averaged value of  $\zeta$ , denoted as  $\hat{\zeta}$ , was determined from these estimates. As in the dry-friction case,  $\hat{\zeta}$  values are presented in Table 1. The  $\hat{\zeta}$  values presented in Table 1 are also consistent, with a standard deviation of 3.72%. Finally, an averaged value of  $\hat{\zeta}$ , denoted as  $\hat{\zeta}_{avg}$ , was obtained which was equal to 0.0320. This value is close to the reference value  $\zeta_{ref}(=0.0298)$ , and the error of  $\hat{\zeta}_{avg}$ , based on  $\zeta_{ref}$ , is 7.5%, slightly larger than that of  $\hat{x}_{kavg}$ . The trend that the  $x_k$  estimate is more accurate than the  $\zeta$  estimate differs from observations made in the numerical study performed in this study and in other experimental studies conducted previously Refs. [6,7,17]. Nonetheless, based on the identifications conducted, it was found that while both the viscous and dry-friction damping seem to be overestimated, the inaccuracy are tolerable.

In order to crosscheck the identification results obtained using the newly proposed method, the displacement-decrement method was applied to the same set of data. The estimates obtained from the displacement-decrement method were denoted as  $x_k^*$  and  $\zeta^*$  in Table 1. Similar to the acceleration-decrement case, many estimates were averaged to produce five individual identifications for each test shown in Fig. 4. These results were then averaged again to determine the final estimate for the whole set of data. To that end,  $\zeta_{avg}^*=0.0307$  with a standard deviation of 4.51%, whereas  $x_{kavg}^*=0.160$  with a standard deviation of 10.1%, representing the final estimations corresponding to the whole set of data obtained from the displacement-decrement method. These data are also listed in Table 1. It can be found that both  $\zeta_{avg}^*$  and  $x_{kavg}^*$  are reliably close to the reference values ( $\zeta_{ref}, x_{kref}$ ) with the error of  $\zeta_{avg}^*$  equal to 3.0% while the error of  $x_{kavg}^*$  equal to 10.2%. Here, the estimate of viscous damping is more accurate than that of the dry friction. Additionally,  $\zeta_{avg}^*$  and  $x_{kavg}^*$  agree well with  $\hat{\zeta}_{avg}$  and  $\hat{x}_{kavg}$ . The error of viscous and dry-friction types of damping between the acceleration- and displacement-decrement method are below 5.0%.

Unlike the acceleration-decrement case, the displacement-decrement method estimates  $x_k$  in accordance with the extracted knowledge of  $\zeta$ . Therefore, the errors of  $\zeta$  estimates could be propagated into those of  $x_k$  estimates. This might be the reason that the error of  $x_{kavg}^*$  based on the reference value is higher than that of  $\zeta_{avg}^*$ .

Thus, it has been shown that the results estimated from the acceleration-decrement method are reliably close to those obtained from the isolated cases and the displacement-decrement approach. Meanwhile, both the displacement- and acceleration-decrement method have been proved to be effective in identifying the combined-damping effects from the experimental data. How to choose a more appropriate method from these two might depend on the characteristics of the system and the feasibility of the measuring devices.

Finally, to evaluate the overall quality of the identification obtained from the acceleration-decrement method of the present damping parameters, the identified mass–spring system was simulated. Fig. 6 illustrates a comparison between the experimental free responses with combined damping and the simulated responses with damping parameters obtained from the proposed method. To simulate, Eq. (1) was numerically integrated with the following parameter values:  $m = 2.42$  kg,  $k = 2310$  N/m,  $\hat{c} = 4.79$  Ns/m ( $\hat{\zeta}_{\text{avg}} = 0.0320$ ),  $\hat{f}_k = 0.351$  N ( $\hat{x}_{k\text{avg}} = 0.152$ ). The frequency of oscillation was 30.90 rad/s. Note that to plot the data correctly, the phase angle between displacement and acceleration sensors need to be accounted for [21]. In this study, the phase angle, leading by accelerometer, was about 0.216 rad.

The comparison is visually quite good. This is true for both the displacement and acceleration signals. In fact, satisfactory results could also be achieved when the estimated damping parameters corresponding to the displacement-decrement method were employed. Thus, an interpretation might be that, in this case, the Coulomb plus viscous model with the estimated

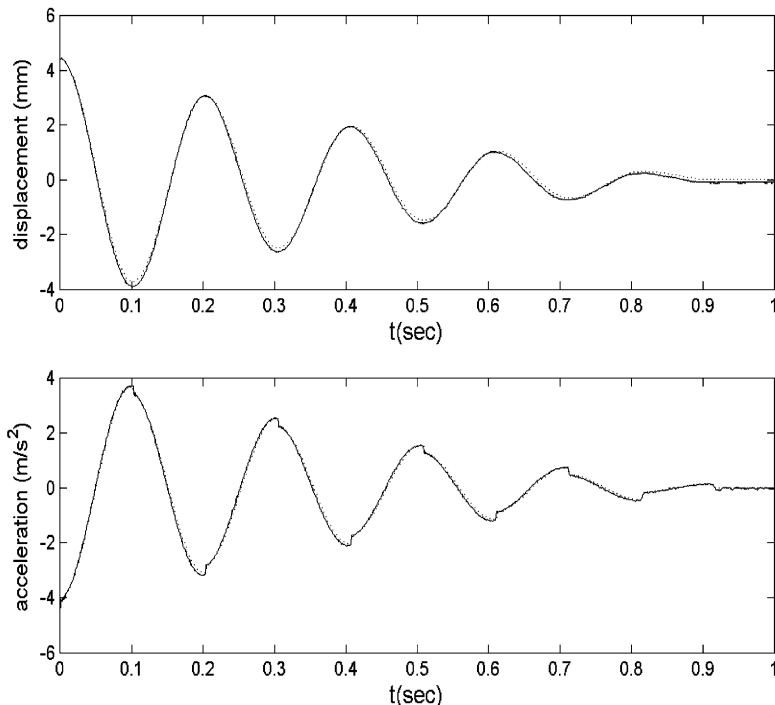


Fig. 6. The solid line shows free-vibration displacement and acceleration responses of the experimental system with both eddy-current and dry damping engaged. Superimposed is a dotted line representing numerical simulation which incorporated the averaged damping parameters obtained from the acceleration-decrement method.

damping parameters fit the experimental system well with regard to its physical damping mechanism. One can still speculate the sources of error though. For example, there might be error pertaining to the assumption of constant sliding friction. In fact, many friction models incorporate velocity dependence. There may also be some variation in the normal load, which can cause error in dry-friction estimation.

## 5. Conclusions

This study proposes new damping-identification schemes, which are capable of extracting damping information from free acceleration decrements of a linear single dof vibratory system. The analytical derivations, numerical verifications and experimental validations are all included. Separate identification equations suitable for the viscous and dry-friction damping estimation are provided. According to the identification algorithms, the inaccuracy occurred in one type of damping will not affect that of another. Numerical verifications illustrate that the damping estimates can be very accurate provided the resolutions of acceleration measurement are high. In the experimental validations, the results obtained from the proposed method are compared with those obtained from the isolated-damping tests and the displacement-decrement method to show the effectiveness and reliability of the new method. It is found that the new method provides reliable estimates without discriminating the type of damping. The displacement-decrement method extracts damping estimates, which agree well with the result obtained from the new method. To solve the problem caused by the irregularity of the raw acceleration signal, a five-point moving average process is taken to smoothen the data.

## Acknowledgements

The author is grateful for the support from National Science Council of Taiwan (NSC89 2212-E-131-001) and valuable discussions from Professor Brian F. Feeny of Michigan State University, USA.

## References

- [1] H.L.F. Helmholtz, *On the Sensations of Tone as Physiological Basis for the Theory of Music*, Dover, New York; 1954, p. 406 (translation by A.J. Ellis of *Die Lehre von den Tonempfindungen*, 4th ed., 1877; 1st ed., 1863).
- [2] Lord Rayleigh, *The Theory of Sound*, Vol. 1, Dover Publications, New York, 1877 (re-issued 1945, pp. 46–51).
- [3] H. Lorenz, *Lehrbuch der Technischen Physik. Erster Band: Technische Mechanik Starrer Gebilde*, Verlag von Julius Springer, Berlin, 1924.
- [4] L.S. Jacobsen, R.S. Ayre, *Engineering Vibrations*, McGraw-Hill, New York, 1958.
- [5] A. Watari, *Kikai-rikigaku*, Kyouritsu, 1969.
- [6] B.F. Feeny, J.-W. Liang, A decrement method for the simultaneous estimation of Coulomb and viscous friction, *Journal of Sound and Vibration* 195 (1996) 149–154.

- [7] J.-W. Liang, B.F. Feeny, Identifying Coulomb and viscous friction from free-vibration decrements, *Nonlinear Dynamics* 16 (1998) 337–347.
- [8] P. Dahl, A solid friction model, Technical Report Tor-0158(3197-18)-1, Aerospace Corp., El Segundo, CA, 1968.
- [9] C. Canudas de Wit, H. Olsson, K.J. Astrom, P. Lischinsky, A new model for control of system with friction, *IEEE Transactions on Automatic Control* 40 (1995) 419–425.
- [10] A. Harnoy, B. Friedland, H. Rachoor, Modeling and simulation of elastic and friction forces in lubricated bearing for precise motion control, *Wear* 172 (1994) 155–165.
- [11] J.-W. Liang, B.F. Feeny, Dynamical friction behavior in a forced oscillator with a compliant contact, *Journal of Applied Mechanics* 65 (1998) 250–257.
- [12] B. Armstrong-Hélouvy, P. Dupont, C. Canudas De Wit, A survey of models analysis tools and compensation methods for the control of machines with friction, *Automatica* 30 (1994) 1083–1138.
- [13] A.A. Polycarpou, A. Soom, Two-dimensional models of boundary and mixed friction at a line contact, *Journal of Tribology* 117 (1995) 178–184.
- [14] A. Ruina, Constitutive relations for frictional slip, in: Z. Bazant (Ed.), *Mechanics of Geomaterials*, Wiley, New York, 1985, pp. 169–187.
- [15] P.E. Dupont, P.S. Kasturi, Experimental investigation of friction dynamics associated with normal load, *Proceedings of the 1995 Design Engineering Technical Conference*, ASME DE-Vol. 84-1, New York, 1995, pp. 1109–1116.
- [16] A.A. Pervozvanski, C. Canudas-de-Wit, Asymptotic analysis of the dither effect in systems with friction, *Automatica* 38 (2002) 105–113.
- [17] S.W. Shaw, On the dynamic response of a system with dry friction, *Journal of Sound and Vibration* 108 (1986) 305–325.
- [18] B.F. Feeny, F.C. Moon, Chaos in a forced dry-friction oscillator: experiments and numerical modeling, *Journal of Sound and Vibration* 170 (1994) 303–323.
- [19] J.P. Meijaard, Efficient numerical integration of the equations of motion of non-smooth mechanical systems, *Applied Mathematics and Mechanics* 77 (1997) 419–428.
- [20] P. Soong, P. Kraus, V. Kumar, P. Dupont, Analysis of rigid-body dynamic models for simulation of systems with frictional contacts, *Journal of Applied Mechanics* 68 (2001) 118–128.
- [21] J.-W. Liang, B.F. Feeny, A comparison between direct and indirect friction measurements in a forced oscillator, *Journal of Applied Mechanics* 65 (1998) 783–786.